

Homogeneous broadening and hyperfine structure of optical transitions in $\text{Pr}^{3+}:\text{Y}_2\text{SiO}_5$

R. W. Equall and R. L. Cone

Physics Department, Montana State University, Bozeman, Montana 59717

R. M. Macfarlane

IBM Almaden Research Center, 650 Harry Road, San Jose, California 95120

(Received 1 February 1995; revised manuscript received 20 March 1995)

Contributions to the homogeneous linewidth of the ${}^3H_4(1) \rightarrow {}^1D_2(1)$ transition for the two crystallographic sites of Pr^{3+} in Y_2SiO_5 have been investigated using photon echoes. The effects of excitation-intensity-dependent dephasing or instantaneous diffusion were systematically studied to allow accurate determination of the optical resonance widths. Homogeneous linewidths of 2.8 kHz (site 1) and 1 kHz (site 2) were measured with no applied magnetic field and with sufficiently low laser intensity to minimize the effects of instantaneous diffusion. Using the same excitation intensity, widths of 2.1 kHz (site 1) and 0.85 kHz (site 2) were obtained with an applied magnetic field of 77 G, demonstrating a significant contribution of ${}^{89}\text{Y}$ nuclear-spin fluctuations to the zero-field homogeneous linewidth. Extrapolation to zero excitation intensity yielded optical resonance widths that were only slightly narrower than the measured values. Optically detected nuclear magnetic resonance measurements determined the hyperfine structure of the 3H_4 ground state for each site; the hyperfine levels of the lowest component of the 1D_2 manifold for each site were determined using photon echo nuclear double resonance. The relatively large oscillator strength of 3×10^{-7} for a rare-earth ion, in conjunction with long dephasing times makes this material a useful candidate for demonstration of time-domain signal processing and optical data storage.

I. INTRODUCTION

The measurement of long optical dephasing times (T_2) of rare-earth ions provides one of the most sensitive probes of the dynamical behavior of solids at low temperatures.¹ At the same time, these and related measurements enable a very high resolution (kHz–MHz) spectroscopic determination of the effect of external perturbations. In applications to time-domain information storage and processing, the dephasing or coherence time T_2 plays a key role by limiting the length of data strings that can be manipulated.^{2–8}

At temperatures below about 2 K, dephasing times of optical transitions from the ground state to metastable levels in rare-earth-doped crystals are usually limited by nuclear-spin fluctuations. To probe the limits on such mechanisms, a number of studies have been made on materials where the near-neighbor anions have zero nuclear spin (e.g., oxides^{9–13} and silicates^{14,15}) and where the other constituent ions have either small magnetic moments or a low abundance of isotopes with nonzero nuclear spin. These studies have been very successful, resulting in several observations of subkilohertz homogeneous optical linewidths.^{10,14,15} We recently reported the measurement of a 122 Hz wide optical resonance in $\text{Eu}^{3+}:\text{Y}_2\text{SiO}_5$ —the narrowest yet observed in a solid and limited only by the population decay time T_1 .¹⁵ The Y_2SiO_5 host is an ideal one in many ways, as large crystals of good optical quality can now be produced, primarily as a result of the demand for its use as a laser material.¹⁶

Here we describe an investigation of optical dephasing of the Pr^{3+} ion in Y_2SiO_5 . As in the case of $\text{Eu}^{3+}:\text{Y}_2\text{SiO}_5$ ¹⁵ we find two contributions to T_2 —one

that is magnetic in origin, involving magnetic-field-dependent ${}^{89}\text{Y}$ nuclear-spin fluctuations, and another that is due to field-independent population decay. For site 2 where the Pr^{3+} ion has the smaller enhanced nuclear moment, the magnetic contribution can be largely suppressed, giving near- T_1 -limited dephasing. For site 1, a contribution of several hundred Hz due to spin-induced dephasing remains. These results were obtained after a detailed investigation of the contribution to dephasing of so-called instantaneous diffusion due to inhomogeneous changes in local fields produced by the excitation pulses. Our studies show that, as in the case of $\text{Eu}^{3+}:\text{Y}_2\text{SiO}_5$, $\text{Pr}^{3+}:\text{Y}_2\text{SiO}_5$ is a useful material for demonstrations of time-domain storage and processing and it has the advantage that Pr^{3+} ions in site 1 have an oscillator strength two orders of magnitude higher than that in the europium material.

II. EXPERIMENT

Y_2SiO_5 is a monoclinic crystal and belongs to the C_{2h}^6 space group with eight molecules per unit cell. Triply ionized rare-earth ions substitute for the Y^{3+} ions and occupy two inequivalent crystallographic sites with no rotational point symmetry (C_1).¹⁷ The crystal used in these studies was commercially produced and contained nominally 0.02% Pr^{3+} . It was determined by x-ray diffraction that all crystal axes made oblique angles relative to the polished faces.

The 3H_4 , 1D_2 , 3P_0 , and 3P_1 levels of $\text{Pr}^{3+}:\text{Y}_2\text{SiO}_5$ were studied via absorption, fluorescence, and fluorescence-excitation spectroscopy. Absorption and fluorescence spectra were recorded at a resolution of 0.5 cm^{-1} using a

SPEX 14018 0.85-meter double monochromator and were calibrated with a uranium hollow cathode lamp. Fluorescence was excited using either a nitrogen-laser-pumped pulsed dye laser or a Coherent 599-21 single-mode cw dye laser. Site-selective fluorescence-excitation spectra were acquired using the pulsed dye laser scanned under computer control while monitoring the fluorescence from the lowest component of the 1D_2 manifold for each site. Fluorescence lifetimes (T_1) for each site were measured by exciting from the ground state $^3H_4(1)$ to the lowest energy component of the 1D_2 manifold, denoted $^1D_2(1)$, for each site with gated cw laser pulses of 1 μ s duration. Emission to the 3H_4 and 3H_5 manifolds was detected with a photomultiplier tube and was averaged with a Tektronix TDS620A digitizing oscilloscope.

The primary goal of this work was the determination of the homogeneous linewidths of the $^3H_4(1) \rightarrow ^1D_2(1)$ transitions for Pr^{3+} in the two sites and of the mechanisms responsible for those widths. Photon echo measurements of the homogeneous linewidths were made with a single-frequency cw dye laser and the apparatus described below. The two-pulse excitation sequence was generated by gating the cw laser with two 80 MHz acousto-optic modulators in series before the sample and focusing with a long focal-length lens of $f = 1$ m to a beam waist of radius $w_0 = 130$ μ m. A third acousto-optic modulator was placed after the sample to reject the transmitted excitation laser pulses, allowing collinear phase-matched detection of the echo with a Hamamatsu R928 photomultiplier tube (PMT). The excitation pulse sequence timing was produced by a computer-controlled Stanford Research Systems DG535 digital delay generator and the echo was averaged using a Tektronix TDS620A digitizing oscilloscope. The echo preparation pulses had a duration of 1 μ s giving a laser bandwidth of ~ 2 MHz, and the excitation power density was varied between ~ 0.4 and 20 W/cm^2 and measured with an electrically calibrated Scientech model 362 thermopile power meter. To avoid spectral holeburning, the laser was repetitively scanned 300 MHz in 250 msec intervals. Photon echo measurements for site 2 (607.934 nm) were performed using an optical path length of 10 mm along a direction that was determined by x-ray diffraction to be at an angle of 20° to the [010] axis. Measurements for site 1 (605.977 nm) were performed in a direction perpendicular to that used for site 2 on a sample of thickness 0.5 mm. All experiments were performed with the crystals immersed in liquid helium that was pumped to 1.4 K.

III. SPECTROSCOPY

Spectroscopic measurements for $\text{Pr}^{3+}:\text{Y}_2\text{SiO}_5$ were reported by Holliday *et al.*,¹⁸ who measured emission from the lowest component of the 1D_2 manifold to the 3H_4 and 3H_5 manifolds at a temperature of 20 K for both crystallographic sites. They also determined the ground-state hyperfine levels using optically detected nuclear magnetic resonance (ODNMR), and the excited-state quadrupole levels for site 1 only, using holeburning which has a lower resolution than photon echo nuclear double resonance (PENDOR) due to laser frequency jitter.

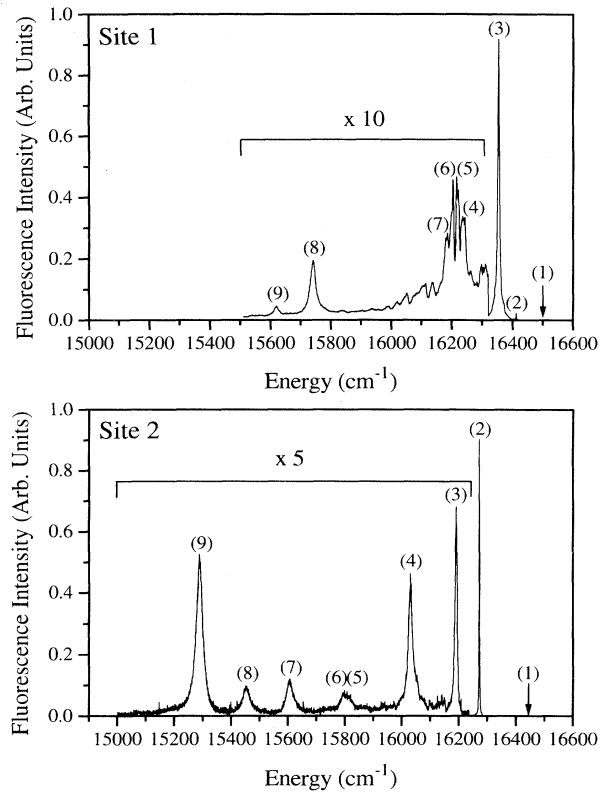


FIG. 1. Fluorescence spectra showing emission from the $^1D_2(1)$ level to the 3H_4 manifold recorded by exciting the $^3H_4(1) \rightarrow ^1D_2(1)$ transition for each crystallographic site of 0.02% $\text{Pr}^{3+}:\text{Y}_2\text{SiO}_5$. Emission from $^1D_2(1) \rightarrow ^3H_4(1)$ is not shown since scatter from the laser saturated the PMT at that energy. Arrows indicate the location of the pump laser which was resonant with the $^3H_4(1) \rightarrow ^1D_2(1)$ transition.

Our fluorescence and ODNMR measurements at 1.4 K gave ground-state crystal-field levels and hyperfine levels that are in good agreement with those of Holliday *et al.*¹⁸ The site selective fluorescence spectra of Fig. 1 show identification of all nine components of the 3H_4 multiplet for each site; however, the peaks labeled (5) and (6) for site 2 and (4) through (7) of site 1 are assigned with a lower degree of certainty than the remaining levels. In addition, we have performed absorption and site-selective excitation measurements on the 1D_2 multiplet and in the region of the 3P_J and 1I_6 multiplets. The $^1D_2(1)$ hyperfine splittings have been measured for both sites with improved resolution.

Our absorption spectra for the 1D_2 , 3P_0 , 3P_1 , and part of the 1I_6 manifolds are shown in Fig. 2. Assignment of the 1D_2 crystal-field levels to the appropriate site was accomplished by recording a laser fluorescence-excitation spectrum while monitoring the fluorescence from the lowest 1D_2 component for each site. No evidence was found for energy transfer between sites.

High-resolution laser absorption spectra for the zero phonon $^3H_4(1) \rightarrow ^1D_2(1)$ transition for each site, shown

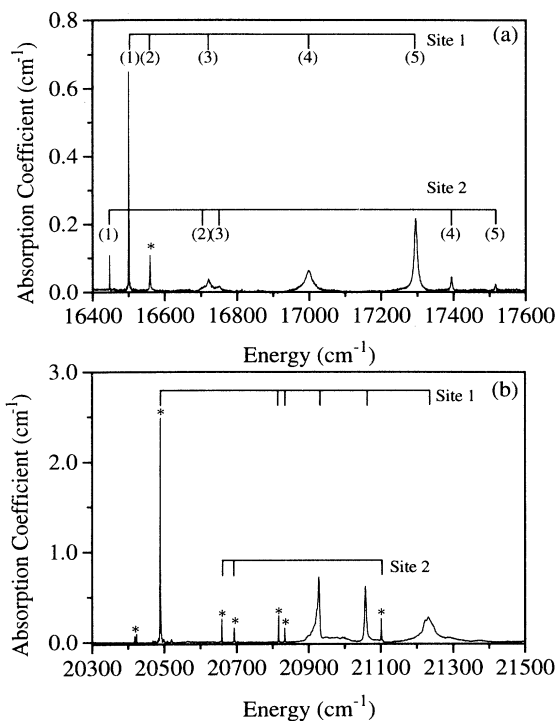


FIG. 2. Absorption spectra showing (a) the 1D_2 multiplet, and (b) the 3P_j and 1I_6 region for both sites of 0.02% $\text{Pr}^{3+}:\text{Y}_2\text{SiO}_5$. Energy and absorption coefficients are each displayed in cm^{-1} units. The widths of the lowest 1D_2 levels and others indicated by * were instrument limited, so the true peak absorption coefficients are proportionately reduced [see Fig. 3 for the actual values for the $^1D_2(1)$ transitions].

in Fig. 3, were measured with the cw dye laser by monitoring the transmitted intensity while scanning the laser over 20 GHz. The inhomogeneous linewidths were 4.4 GHz (site 1) and 2.5 GHz (site 2) full width at half maximum (FWHM). It is worth noting that the inhomogeneous linewidths obtained for our sample are significantly narrower than the 30 GHz (site 1) and 10 GHz (site 2) linewidths reported for the crystal used by Holliday *et al.*¹⁸ Our crystal had peak absorption coefficients of $\alpha = 10 \text{ cm}^{-1}$ (site 1) and $\alpha = 1.3 \text{ cm}^{-1}$ (site 2) centered at 605.977 and 607.934 nm for site 1 and site 2, respectively. The corresponding oscillator strengths are 3×10^{-7} for site 1 and 2×10^{-8} for site 2 for the polarization and propagation direction used here. Sample lengths of 0.5 mm (site 1) and 10 mm (site 2) resulted in an absorption of 40% for site 1 and 73% for site 2.

Fluorescence lifetimes were measured as described in the previous section. The $^1D_2(1)$ lifetimes were $T_1 = 164 \pm 5 \mu\text{s}$ (site 1) and $T_1 = 222 \pm 5 \mu\text{s}$ (site 2). These lifetimes are similar to those observed for other oxide hosts such as YAlO_3 ($T_1 = 180 \mu\text{s}$) and YAG ($T_1 = 230 \mu\text{s}$).

High-resolution radio-frequency measurements of the excited-state hyperfine splittings were made using photon echo nuclear double resonance (PENDOR).¹⁹ The PENDOR measurements were performed using the photon

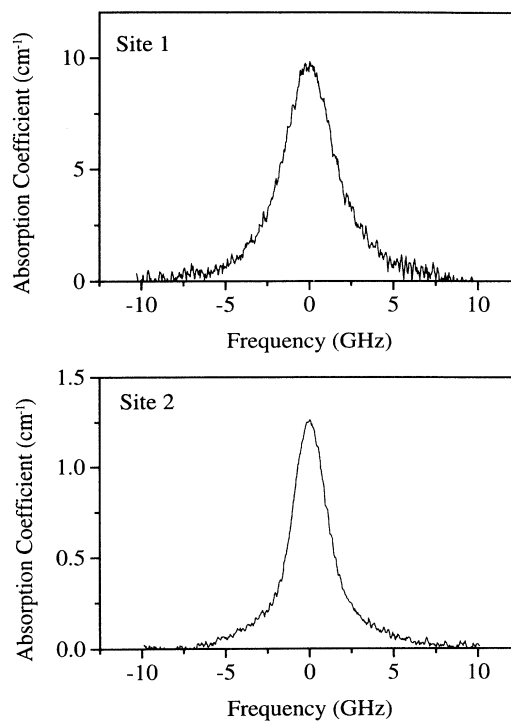


FIG. 3. Absorption coefficient versus frequency for the $\text{Pr}^{3+}:\text{Y}_2\text{SiO}_5$ $^3H_4(1) \rightarrow ^1D_2(1)$ transitions for sites 1 and 2 recorded by monitoring the transmission of a single frequency cw dye laser. Sample orientation is described in the text.

echo apparatus described in the previous section with the addition of a radio-frequency (RF) magnetic field of ~ 1 G applied to the sample with a ten turn copper coil driven by a PTS 500 RF synthesizer and ENI model 411LA 10 watt RF amplifier. The photon echo intensity was monitored at a fixed excitation pulse time delay of 250 μs (site 2) and 100 μs (site 1), while the RF frequency was scanned. When the RF field was resonant with an excited-state or ground-state hyperfine splitting, a large reduction in the photon echo intensity was recorded. Excited state splittings of 4.595 and 4.84 MHz were determined for site 1 from resonances observed experimentally at these frequencies and at the sum frequency, with widths of 30, 18, and 7 kHz, respectively. Resonances were observed only at 2.296 and 4.592 MHz for site 2 (both with widths of ~ 7 kHz), suggesting that the three excited-state Kramer's doublets are equally spaced with separations of 2.296 MHz. These more precise values for site 1 agree with those of Holliday *et al.*¹⁸ to within their experimental error. Values for site 2 were not previously reported. Energy-level diagrams summarizing the energies of the 3H_4 ground-state multiplets and 1D_2 excited-state multiplets are shown in Fig. 4.

The nuclear quadrupole interaction and second-order magnetic hyperfine or "pseudoquadrupole" interaction can be combined^{20,21} to give the effective quadrupole Hamiltonian

$$H_Q = D[I_z^2 - I(I+1)/3] + E(I_x^2 - I_y^2). \quad (1)$$

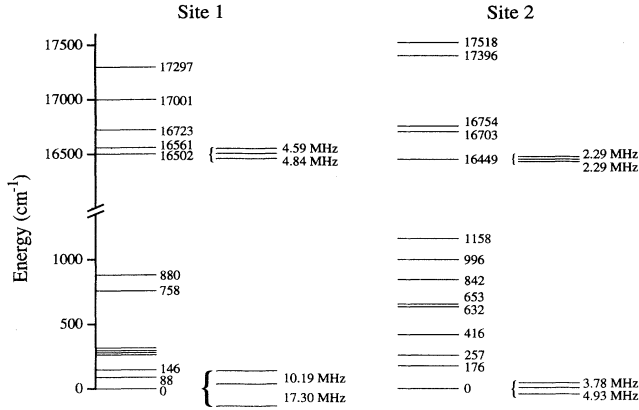


FIG. 4. Energy levels for the 3H_4 ground-state multiplets and 1D_2 excited-state multiplets for the two crystallographic sites of Pr^{3+} in Y_2SiO_5 at 1.4 K. The ordering of the hyperfine splittings for the lowest components of the 3H_4 and 1D_2 multiplets is unknown since our experiments did not determine these.

The measured hyperfine splittings given above were used to calculate the combined quadrupole and second-order-hyperfine coupling constants D and E . Table I summarizes the observed hyperfine splittings and the fitted coupling parameters for the ground and excited states for both crystallographic sites. The signs of D and E are not specified since our experiments did not determine the ordering of the hyperfine levels.

IV. PHOTON ECHO MEASUREMENTS

Homogeneous broadening of optical transitions in rare-earth-doped crystals arises from dynamic perturbations on the transition frequency. The homogeneous linewidth Γ_h can be written as a sum of contributions from several mechanisms:

$$\Gamma_h = \Gamma_{\text{pop}} + \Gamma_{\text{ion-spin}} + \Gamma_{\text{ion-ion}} + \Gamma_{\text{phonon}}, \quad (2)$$

where Γ_{pop} is the contribution from the excited-state population lifetime T_1 , $\Gamma_{\text{ion-spin}}$ is the contribution due to nuclear and electron-spin fluctuations of the host lattice, $\Gamma_{\text{ion-ion}}$ is the contribution from changes in the local environment due to the optical excitation or population relaxation of other ions (so-called instantaneous spectral

diffusion), and Γ_{phonon} includes pure dephasing contributions from temperature-dependent phonon scattering. Room temperature homogeneous linewidths for rare-earth doped systems are typically dominated by Γ_{phonon} , but at low temperatures phonon scattering is frozen out so the Γ_{phonon} term in Eq. (2) is negligible.

The first term Γ_{pop} contains contributions from radiative and nonradiative decay, and establishes the ultimate limit on Γ_h . For the lowest component of multiplets like 1D_2 , below which there is a very large energy gap, the contribution to Γ_{pop} from spontaneous phonon emission is typically very small, leaving radiative decay as the dominant contribution. The “ T_1 limit” for the $Pr^{3+}:Y_2SiO_5$ crystal studied here is calculated from the measured fluorescence lifetimes given in the previous section. Using $\Gamma_{\text{pop}} = 1/(2\pi T_1)$, we found it contributes 970 ± 30 Hz for site 1 and 717 ± 16 Hz for site 2.

The contribution from the second term $\Gamma_{\text{ion-spin}}$ is strongly dependent on the magnetic properties of the host lattice and can vary by at least an order of magnitude from material to material.^{15,22–24} Indeed, Y_2SiO_5 studied here was chosen by Yano, Mitsunaga, and Uesugi¹⁴ to minimize the ion-spin contribution by reducing the nuclear magnetic moments of the ligands to zero (^{16}O), to very small values (^{89}Y) or to low abundance (^{29}Si). In the absence of ion-spin interactions and at extremely low excitation intensities, it is, in principle, possible to reach the limit of the homogeneous linewidth established by population decay as discussed above.

The third term $\Gamma_{\text{ion-ion}}$ has recently been shown^{15,25–34} to make important contributions to any measured value of the linewidth since the measurement process itself can introduce this additional broadening. In an ideal photon echo experiment, an ensemble of isolated two-level ions is “rephased” by the classic two-pulse excitation sequence, removing deterministic inhomogeneous dephasing effects and allowing accurate measurement of the dephasing time T_2 . In real photon echo experiments on crystals, however, the first and second excitation laser pulses cause abrupt and random shifts in the transition frequency of the Pr^{3+} echo ions due to perturbations arising from optical excitation of other Pr^{3+} ions, even at low ion concentrations and low excitation densities such as that used here. When these random “static” frequency shifts are not present throughout the entire echo pulse sequence, they cause rephasing to be incomplete, and therefore they decrease the echo intensity. Since the laser pulses are short compared to $T_2 = 1/(\pi\Gamma_h)$, the laser-induced inhomogeneous frequency shifts are often called instantaneous spectral diffusion. This effect has been studied for various rare-earth-doped materials and can contribute to the homogeneous linewidth through a variety of interaction mechanisms.^{25–34} For ions in singlet states, as for Pr^{3+} here, electrostatic coupling is apparently the most important mechanism for the shifts. The magnitude of the instantaneous diffusion contribution to the linewidth is proportional to the number of excited ions and is therefore directly proportional to the excitation intensity. As a result, the homogeneous linewidth versus excitation intensity must be determined for each material and each set

TABLE I. Hyperfine levels and spin-Hamiltonian parameters for the $^3H_4(1)$ to $^1D_2(1)$ transition for each site of Pr^{3+} in Y_2SiO_5 as measured by ODNMR and PENDOR (in MHz).

	Site 1		Site 2	
	$^3H_4(1)$	$^1D_2(1)$	$^3H_4(1)$	$^1D_2(1)$
δ_1	10.19	4.59	3.78	2.29
δ_2	17.3	4.84	4.93	2.29
$\delta_1 + \delta_2$	27.5	9.43	8.71	4.58
$ D $	4.44	1.36	1.32	0.651
$ E $	0.564	0.425	0.305	0.217

TABLE II. Spectral and relaxation parameters for the ${}^3H_4(1) \rightarrow {}^1D_2(1)$ transition for each site in 0.02% $\text{Pr}^{3+}:\text{Y}_2\text{SiO}_5$.

	Site 1	Site 2
$\lambda[{}^3H_4(1) \rightarrow {}^1D_2(1)]$	605.977 nm	607.934 nm
Γ_{inh}	4.4 GHz	2.5 GHz
T_1	$164 \pm 5 \mu\text{s}$	$222 \pm 5 \mu\text{s}$
$\Gamma_h(T_1) \equiv \Gamma_{\text{pop}}$	$970 \pm 30 \text{ Hz}$	$717 \pm 16 \text{ Hz}$
T_2^a	$152 \mu\text{s}$	$377 \mu\text{s}$
	($\equiv 2100 \text{ Hz}$)	($\equiv 848 \text{ Hz}$)
Γ_h^b	1800 Hz	850 Hz
f	3×10^{-7}	2×10^{-8}
α	10 cm^{-1}	1.3 cm^{-1}

^aFor $H_0 = 77 \text{ G}$.

^bExtrapolated to zero laser intensity for $H_0 = 77 \text{ G}$.

of experimental conditions (for example, each magnetic field) to allow extrapolation to the true zero-intensity homogeneous linewidth to be made. For a given sample, one can minimize the $\Gamma_{\text{ion-ion}}$ contribution by decreasing the sample excitation density (excitation laser intensity), but in doing so, the echo intensity is also reduced. In the present study, our low power measurements (small-pulse-area limit) approached the zero-intensity homogeneous linewidth limit quite closely.

The contributions to the homogeneous linewidth described above have been investigated using two-pulse photon echo measurements. All measurements were made at the center of the inhomogeneous line and with the sample shielded from stray electromagnetic fields by a copper box. Table II summarizes the important spectroscopic and relaxation parameters for Pr^{3+} in Y_2SiO_5 . Echo decays for each site were recorded as a function of excitation power density with the crystal in zero field and in a field of 77 G. The power dependence of the homogeneous linewidth is shown in Fig. 5. The echo decays were always exponential for both sites. The results shown in Fig. 6 are for the lowest excitation intensities used, corresponding to the most challenging experimental conditions.

Dephasing times of $T_2 = 111 \pm 4 \mu\text{s}$ for site 1 and $T_2 = 306 \pm 14 \mu\text{s}$ for site 2 were recorded at the lowest excitation intensities in zero applied magnetic field. These dephasing times correspond to homogeneous linewidths of $2.8 \pm 0.1 \text{ kHz}$ for site 1 and $1.04 \pm 0.05 \text{ kHz}$ for site 2. Extrapolation to zero excitation intensity yielded only a slightly narrower linewidth of 2.4 kHz for site 1 indicating that at the lowest intensities used instantaneous diffusion is adding $\sim 400 \text{ Hz}$. The extrapolated value for site 2 was $1.05 \pm 0.05 \text{ kHz}$, the same as the measured value within the experimental uncertainty, indicating no measurable contribution from instantaneous diffusion for that site at this excitation power density.

Echo decays were also recorded in a field of 77 G to explore the contribution to the linewidth from ${}^{89}\text{Y}$ nuclear-spin fluctuations. The external magnetic field reduced the homogeneous linewidths to $2.1 \pm 0.1 \text{ kHz}$ (site 1) and $0.85 \pm 0.04 \text{ kHz}$ (site 2) at the lowest excitation intensities. As for the zero-field case, extrapolation to zero excitation intensity yielded a slightly narrower linewidth of 1.8 kHz for site 1, with the value for site 2 essentially the same as that measured to within experimental error. Sen-

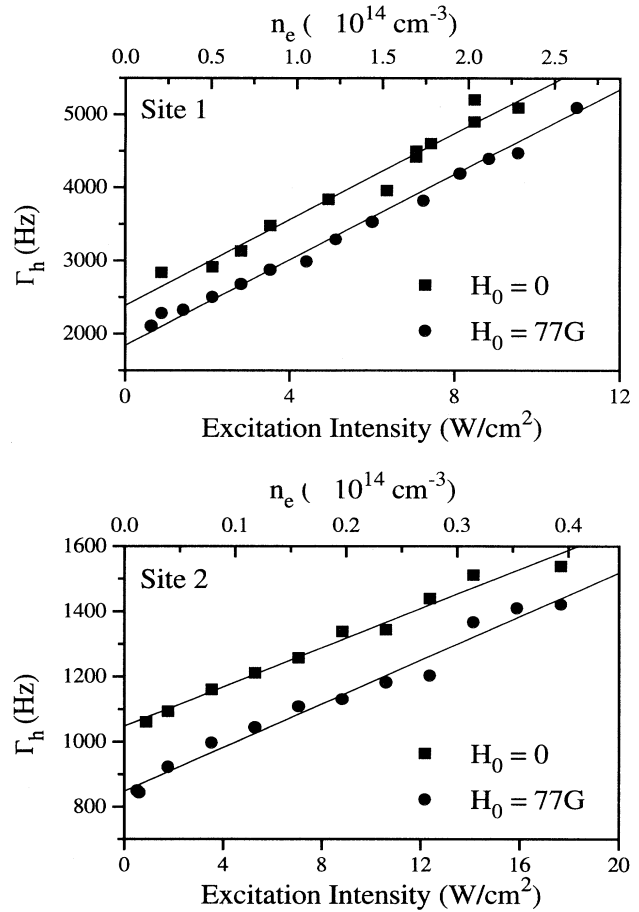


FIG. 5. Dependence of the homogeneous linewidth of the ${}^3H_4(1) \rightarrow {}^1D_2(1)$ transition on excitation power density for site 1 and site 2 showing the contribution from instantaneous diffusion. Both echo preparation pulses had the same intensity and were varied simultaneously. Alternate horizontal axes relate the incident laser excitation power density to the Pr^{3+} ion excitation density n_e calculated using the absorption coefficients of Fig. 3. The slopes of Γ_h vs n_e are similar for the two sites.

sitivity of the homogeneous linewidth to a magnetic field (H_0) indicates nuclear spin-flip-induced dephasing; application of the field modifies the spin dynamics, slowing the ${}^{89}\text{Y}$ mutual nuclear-spin flips thus reducing their contribution to the homogeneous linewidth. In the case of Pr^{3+} in Y_2SiO_5 , the application of the 77 G field reduced the linewidth of site 1 by $\sim 600 \text{ Hz}$ and site 2 by $\sim 200 \text{ Hz}$. In the case of site 2, the extrapolated (or measured) linewidth of 0.85 kHz is very close to the 0.72 kHz limit established by population decay. The residual 130 Hz is nearly within the combined experimental and fitting uncertainty of $\sim 80 \text{ Hz}$, although it is expected that a small contribution ($\sim 50 \text{ Hz}$) due to ${}^{89}\text{Y}$ nuclear-spin flips is still present. The extrapolated value of 1.8 kHz for site 1 is $\sim 800 \text{ Hz}$ broader than the T_1 limit. At least some of this additional broadening is due to effects of ${}^{89}\text{Y}$ mutual spin flips still present at a field intensity of 77 G. The contribution to the homogeneous linewidth due to ${}^{29}\text{Si}$ nuclear-spin fluctuations is expected to be significantly smaller than the contribution from ${}^{89}\text{Y}$. The magnetic moment of ${}^{29}\text{Si}$ ($-0.55\mu_N$) is \sim four times that of ${}^{89}\text{Y}$

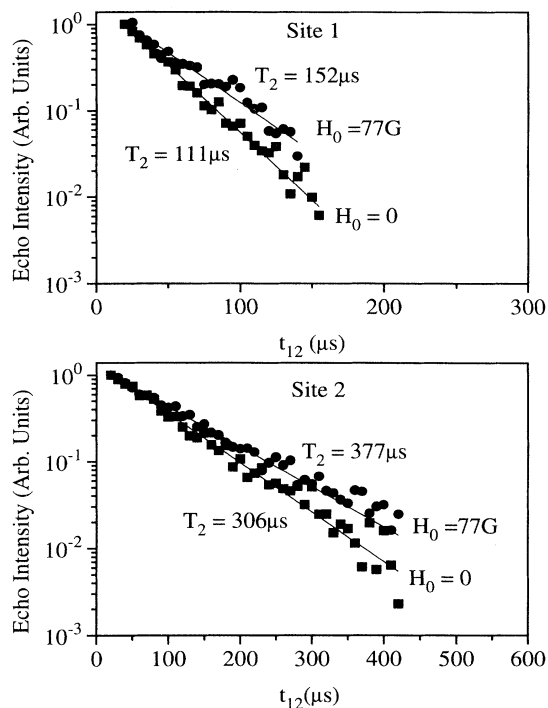


FIG. 6. Photon echo decays on the ${}^3H_4(1) \rightarrow {}^1D_2(1)$ transition of $\text{Pr}^{3+}:\text{Y}_2\text{SiO}_5$ at 1.4 K. The excitation density was 0.64 W/cm^2 for site 1 and 0.52 W/cm^2 for site 2. The straight lines are exponential fits to the decays yielding the dephasing times shown. The magnetic field H_0 was applied with a Helmholtz coil.

($-0.14\mu_N$), but the concentration of the former is ~ 40 times lower, resulting in a $\text{Pr}^{3+}\text{-}^{29}\text{Si}$ coupling strength that is about an order of magnitude smaller than for ${}^{89}\text{Y}$. In addition, the dephasing due to ${}^{29}\text{Si}$ is expected to be less effective since the mutual spin-flip rates for the ${}^{29}\text{Si}$ will be substantially lower than for ${}^{89}\text{Y}$.

We recently reported an observation of optical line broadening by ${}^{89}\text{Y}$ spin fluctuations for the ${}^5D_0 \rightarrow {}^7F_0$ transition of $\text{Eu}^{3+}:\text{Y}_2\text{SiO}_5$.¹⁵ The contribution for each site was $\sim 100 \text{ Hz}$. This is considerably smaller than the contributions of $\sim 1.4 \text{ kHz}$ for site 1 and $\sim 300 \text{ Hz}$ for site 2 observed here for Pr^{3+} ions. The larger contributions for Pr^{3+} are expected, however, since the enhanced nuclear magnetic moments^{35,36} in the Pr^{3+} ground and excited states are large compared to Eu^{3+} where the magnetic moment is quenched in the ground state and very small in the excited state. The Pr^{3+} ions also exhibit significant differences in the yttrium spin contribution to dephasing for each site; this is presumably a consequence of the differences in the crystal fields at the two sites. Site 1 has a ground-state crystal-field splitting of 88 cm^{-1} between the two lowest components of the 3H_4 manifold, while site 2 has a splitting of 176 cm^{-1} . Since the enhanced magnetic moment arises from the second-order magnetic hyperfine interaction, which is inversely proportional to this energy difference, a larger enhanced moment is expected for site 1 than for site 2.

When comparing the $\Gamma_{\text{ion-ion}}$ instantaneous diffusion

contributions to the dephasing for the two crystallographic sites, it is appropriate to recall²⁹ that $\Gamma_{\text{ion-ion}}$ is proportional to the excitation density and to changes in electric dipolar coupling between Pr^{3+} ions as neighbors undergo transitions between the ground and excited states. When the Pr^{3+} ion excitation density n_e is chosen as the horizontal axis for the Γ_h versus laser excitation power density data, as shown on the alternate scales in Fig. 5, differences in slope arising from the $\Gamma_{\text{ion-ion}}$ contribution to Γ_h reflect differences in dipolar interactions and angular coordination to near and distant neighbors for the two sites. Using the measured absorption coefficients for sites 1 and 2, an effective beam area based on the top-hat approximation $A = \pi w_0^2/2$, and the methods outlined by Liu and Cone,²⁹ the instantaneous diffusion slopes were found to be $1.2 \times 10^{-11} \text{ Hz cm}^3$ for site 1 and $1.4 \times 10^{-11} \text{ Hz cm}^3$ for site 2. When experimental uncertainty is taken into account, these values are essentially the same, a result that perhaps arises at least in part from the angular averaging that occurs in the summation over large numbers of ions in calculations of $\Gamma_{\text{ion-ion}}$. Information on the dipole moments is not available, precluding a numerical estimate of $\Gamma_{\text{ion-ion}}$ at this time. The absorption coefficient for site 1 is approximately ten times larger than site 2, but there is no relationship between the off-diagonal electric dipole moments that determine the optical oscillator strength and the diagonal moments for the ground and excited states that are involved in the instantaneous diffusion. Future studies should include Stark effect measurements to obtain the dipole moment differences.

V. CONCLUSION

In summary, the spectroscopic properties and dephasing mechanisms of Pr^{3+} ions in Y_2SiO_5 have been investigated in detail. We have extended existing spectroscopic information by reporting a high-resolution determination of the hyperfine levels for the lowest-energy component of the 1D_2 excited state for both crystallographic sites. Upper crystal-field components of the 1D_2 multiplet were also identified and assigned to the appropriate site, and absorption spectra were presented for higher multiplets which had not been previously reported.

The homogeneous linewidth of the transition from the ${}^3H_4(1)$ ground state to the ${}^1D_2(1)$ excited state has been measured for the two crystallographic sites using photon echoes. The contributions to the homogeneous linewidths were identified for each site by detailed characterization of the effects of excitation-intensity-dependent dephasing. At a temperature of 1.4 K, each site had two contributions to the linewidth: a small contribution from ${}^{89}\text{Y}$ nuclear-spin fluctuations and a larger contribution from population decay. The host crystal Y_2SiO_5 has again been shown to yield a narrower optical resonance for a specific ion, in this case Pr^{3+} , than for any previously reported host. It is also clear, from this and other studies, that any measurement of a homogeneous linewidth using photon echoes requires careful identification of the instantaneous diffusion contribution in order to characterize the intrinsic optical resonance width.

ACKNOWLEDGMENTS

The research at Montana State University was supported in part by Scientific Materials Corporation, Bozeman, Montana, NASA EPSCoR (Grant No. NCCW0058),

NSF EPSCoR-ESI (Grant No. OSR-93536541), NSF EPSCoR III (Grant No. OSR-9350546), and AFOSR (Grant No. F49620-93-1-0530DEF). We also acknowledge the help of Yongchen Sun with the ODNMR and PENDOR experiments.

- ¹R. M. Macfarlane and R. M. Shelby, in *Spectroscopy of Solids Containing Rare Earth Ions*, edited by A. A. Kaplyanskii and R. M. Macfarlane (North-Holland, Amsterdam, 1987), pp. 55–184.
- ²*Persistent Spectral Hole-Burning: Science and Applications*, edited by W. E. Moerner, Topics in Current Physics, Vol. 44 (Springer, Berlin, 1988).
- ³T. W. Mossberg, *Opt. Lett.* **7**, 77 (1982).
- ⁴W. R. Babbitt and T. W. Mossberg, *Opt. Commun.* **65**, 185 (1988).
- ⁵M. Mitsunaga, R. Yano, and N. Uesugi, *Opt. Lett.* **16**, 1890 (1991).
- ⁶T. W. Mossberg, *Opt. Lett.* **17**, 535 (1992).
- ⁷Y. S. Bai and R. Kachru, *Opt. Lett.* **18**, 1189 (1993).
- ⁸W. R. Babbitt and J. A. Bell, *Appl. Opt.* **33**, 1538 (1994).
- ⁹R. M. Macfarlane, R. M. Shelby, and R. L. Shoemaker, *Phys. Rev. Lett.* **43**, 1726 (1979).
- ¹⁰R. M. Macfarlane and R. M. Shelby, *Opt. Commun.* **39**, 169 (1981).
- ¹¹M. K. Kim and R. Kachru, *Phys. Rev. B* **44**, 9826 (1991).
- ¹²M. Mitsunaga, R. Yano, and N. Uesugi, *Phys. Rev. B* **45**, 12 760 (1992).
- ¹³R. M. Shelby, A. C. Tropper, R. T. Harley, and R. M. Macfarlane, *Opt. Lett.* **18**, 1958 (1993).
- ¹⁴R. Yano, M. Mitsunaga, and N. Uesugi, *Opt. Lett.* **16**, 1884 (1991).
- ¹⁵R. W. Equall, Y. Sun, R. L. Cone, and R. M. Macfarlane, *Phys. Rev. Lett.* **72**, 2179 (1994).
- ¹⁶C. D. Brandle, A. J. Valentino, and G. W. Berkstresser, *J. Cryst. Growth* **79**, 308 (1986); R. Beach, M. D. Shinn, L. Davis, R. W. Solarz, and W. Krupke, *IEEE J. Quant. Electron.* **26**, 1405 (1990); C. Li, R. Moncorge, J. C. Souriau, and C. H. Wyon, *Opt. Commun.* **101**, 356 (1993).
- ¹⁷B. A. Maximov, Yu. A. Charitonov, V. V. Ilyikhin, and N. B. Belov, *Dok. Akad. Nauk. SSSR* **183**, 1072 (1968) [*Sov. Phys. Dokl.* **13**, 1188 (1969)].
- ¹⁸Keith Holliday, Mauro Croci, Eric Vauthey, and Urs P. Wild, *Phys. Rev. B* **47**, 14 741 (1993); [Low resolution measurements without site discrimination were reported for 77 and 300 K by N. V. Kuleshov, V. P. Mikhailov, S. A. Radkevich, V. N. Boikov, D. S. Umreiko, and B. I. Minkov, *Opt. Spektrosk.* **77**, 244 (1994) {*Opt. Spectrosc.* **77**, 220 (1994)}.]
- ¹⁹P. Hu, R. Leigh, and S. R. Hartmann, *Phys. Lett. A* **40**, 164 (1972).
- ²⁰J. M. Baker and B. Bleaney, *Proc. R. Soc. London Ser. A* **245**, 156 (1958).
- ²¹M. A. Teplov, *Zh. Eksp. Teor. Fiz.* **53**, 1510 (1968) [*Sov. Phys. JETP* **26**, 872 (1968)].
- ²²R. M. Macfarlane, C. S. Yannoni, and R. M. Shelby, *Opt. Commun.* **32**, 101 (1980).
- ²³R. M. Shelby and R. M. Macfarlane, *Phys. Rev. Lett.* **45**, 1098 (1980).
- ²⁴S. Kröll, E. Y. Xu, and R. Kachru, *Phys. Rev. B* **44**, 30 (1991).
- ²⁵D. R. Taylor and J. P. Hessler, *Phys. Lett.* **50A**, 205 (1974).
- ²⁶G. K. Liu, M. F. Joubert, R. L. Cone, and B. Jacquier, *J. Lumin.* **38**, 34 (1987).
- ²⁷J. Huang, J. M. Zhang, A. Lezama, and T. W. Mossberg, *Phys. Rev. Lett.* **63**, 78 (1989).
- ²⁸G. K. Liu, R. L. Cone, M. F. Joubert, B. Jacquier, and J. L. Skinner, *J. Lumin.* **45**, 387 (1990).
- ²⁹G. K. Liu and R. L. Cone, *Phys. Rev. B* **41**, 6193 (1990).
- ³⁰J. Huang, J. M. Zhang, and T. W. Mossberg, *Opt. Commun.* **75**, 29 (1990).
- ³¹S. Kröll, E. Y. Xu, M. K. Kim, M. Mitsunaga, and R. Kachru, *Phys. Rev. B* **41**, 11 568 (1990).
- ³²R. Yano, M. Mitsunaga, and N. Uesugi, *J. Opt. Soc. Am. B* **9**, 992 (1992).
- ³³Y. S. Bai and R. Kachru, *Phys. Rev. B* **46**, 13 753 (1992).
- ³⁴S. B. Altner, U. P. Wild, and M. Mitsunaga, *Chem. Phys. Lett.* **237**, 406 (1995).
- ³⁵B. Bleaney, *Physica* **69**, 317 (1973).
- ³⁶A. Abragam and B. Bleaney, *Proc. R. Soc. London Ser. A* **387**, 221 (1983).